Published in final edited form as:
Am J Ophthalmol. 2022 December ; 244: 98–116. doi:10.1016/j.ajo.2022.08.013.

Baseline Microperimetry and OCT in the RUSH2A Study: Structure-Function Association and Correlation with Disease Severity

Eleonora M. Lad[1], **Jacque L. Duncan**[2], **Wendi Liang**[3], **Maureen G. Maguire**[3], **Allison R. Ayala**[3], **Isabelle Audo**[4,5], **David G. Birch**[6], **Joseph Carroll**[7], **Janet K. Cheetham**[8], **Todd A. Durham**[8], **Abigail T. Fahim**[9], **Jessica Loo**[10], **Zengtian Deng**[10], **Dibyendu Mukherjee**[10], **Elise Heon**[11], **Robert B. Hufnagel**[12], **Bin Guan**[12], **Alessandro Iannaccone**[1], **Glenn J. Jaffe**[1], **Christine N. Kay**[13], **Michel Michaelides**[14], **Mark E. Pennesi**[15], **Ajoy Vincent**[11], **Christina Y. Weng**[16], **Sina Farsiu**[1,10],
Foundation Fighting Blindness Consortium Investigator Group[*]

[1]Duke University Medical Center, Department of Ophthalmology, Durham, NC

[2]University of California, San Francisco, San Francisco, CA

[3]Jaeb Center for Health Research, Tampa, FL

[4]Institut de la Vision, Sorbonne Université, INSERM, CNRS, Paris, France

[5]Centre Hospitalier National d'Ophtalmologie des Quinze-Vingts, INSERM-DGOS CIC1423, Paris, France

[6]Retina Foundation of the Southwest, Dallas, TX

[7]Medical College of Wisconsin, Milwaukee, WI

[8]Foundation Fighting Blindness, Columbia, MD

[9]Kellogg Eye Center, University of Michigan, Ann Arbor, MI

[10]Duke University, Department of Biomedical Engineering, Durham, NC

[11]University of Toronto and Hospital for Sick Children, Toronto, Canada

[12]National Eye Institute, Bethesda, MD

[13]Vitreoretinal Associates, Gainesville, FL

[14]Moorfields Eye Hospital and UCL Institute of Ophthalmology, London, United Kingdom

Corresponding Author: Allison Ayala; Jaeb Center for Health Research; 15310 Amberly Drive, Tampa, FL, 33647; ffbcorrespauth@jaeb.org.

[*]The comprehensive list of FFB Consortium Investigator Group members participating in this protocol was previously published in Duncan JL, Liang W, Maguire MG, et al. Baseline Visual Field Findings in the RUSH2A Study: Associated Factors and Correlation with Other Measures of Disease Severity. *Am J Ophthalmol*. 2020

Meeting Presentations: This manuscript was presented in part at the Retina Society 2020, the Macula Society 2021, and ARVO 2021.

Supplemental Material available at AJO.com.

[15]Casey Eye Institute - Oregon Health & Science University, Portland, OR

[16]Baylor College of Medicine, Houston, TX

Abstract

Purpose: To investigate baseline mesopic microperimetry (MP) and spectral domain optical coherence tomography (OCT) in the Rate of Progression in *USH2A*-related Retinal Degeneration (RUSH2A) study.

Design: Natural history study

Setting: 16 clinical sites in Europe and North America

Study Population: Participants with Usher syndrome type 2 (USH2) (N=80) or autosomal recessive nonsyndromic RP (ARRP) (N=47) associated with biallelic disease-causing sequence variants in *USH2A*.

Observation Procedures: General linear models were used to assess characteristics including disease duration, MP mean sensitivity and OCT intact ellipsoid zone (EZ) area. The associations between mean sensitivity and EZ area with other measures, including best corrected visual acuity (BCVA) and central subfield thickness (CST) within the central 1 mm, were assessed using Spearman correlation coefficients.

Main Outcome Measures: Mean sensitivity on MP; EZ area and CST on OCT

Results: All participants (N=127) had OCT, while MP was obtained at selected sites (N= 93). Participants with Usher syndrome type 2 (USH2, N=80) and nonsyndromic autosomal recessive Retinitis Pigmentosa (ARRP, N=47) had the following similar measurements: EZ area (median (interquartile range [IQR]): 1.4 (0.4, 3.1) mm^2 vs 2.3 (0.7, 5.7) mm^2) and CST (median (IQR): 247 (223, 280) μm vs 261 (246, 288), and mean sensitivity (median (IQR): 3.5 (2.1, 8.4) dB vs 5.1 (2.9, 9.0) dB). Longer disease duration was associated with smaller EZ area (P<0.001) and lower mean sensitivity (P=0.01). Better BCVA, larger EZ area, and larger CST were correlated with greater mean sensitivity (r>0.3 and P<0.01). Better BCVA and larger CST were associated with larger EZ area (r>0.6 and P<0.001).

Conclusions: Longer disease duration correlated with more severe retinal structure and function abnormalities, and there were associations between MP and OCT metrics. Monitoring changes in retinal structure-function relationships during disease progression will provide important insights into disease mechanism in *USH2A*-related retinal degeneration.

Table of Contents Statement

The international, natural history study Rate of Progression in *USH2A*-related Retinal Degeneration (RUSH2A) enrolled 80 participants with Usher syndrome type 2 and 47 with autosomal recessive retinitis pigmentosa associated with biallelic variants in the *USH2A* gene. At baseline, longer disease duration correlated with more severe retinal structure (smaller ellipsoid zone area) and functional abnormalities (lower mean retinal sensitivity on microperimetry). A structure-function association was identified between microperimetry and optical coherence tomography metrics.

Usher syndrome is the leading cause of autosomal recessive deaf-blindness and is genetically heterogeneous.[1,2] The most common form of Usher syndrome (56–67%) is Usher syndrome type 2 (USH2), with mild/moderate congenital hearing impairment and inherited retinal degeneration (IRD) beginning in the first or second decade.[3,4] The gene most commonly associated with USH2 is *USH2A*, which accounts for 57–80% of USH2 patients.[5,6] Retinitis Pigmentosa (RP) in *USH2A* shows primary rod and secondary cone photoreceptor degeneration followed by retinal pigment epithelial (RPE) degeneration.[7] *USH2A* mutations result in a wide phenotypic spectrum, with normal function in some patients, especially in the macula.[8] *USH2A* variants can also lead to IRD without hearing loss and represent the most common cause of nonsyndromic autosomal recessive RP (ARRP).[5]

USH2A-related natural history studies of retinal structure and function are limited. Earlier functional data was obtained with older techniques (Snellen acuity charts and Goldmann kinetic perimetry) in several single-center studies that lacked robust genotyping.[9,10] A study of 225 patients with *USH2A*-related IRD showed that individuals with USH2 had more severe symptoms and earlier visual loss than patients with ARRP, likely related to the difference in severity of causative genetic variants.[11] However, this study lacked detailed retinal phenotype data obtained using quantitative, high-resolution modalities for evaluation of structural and functional loss.

Prior studies did not perform assessments using current evaluation modalities, including spectral-domain optical coherence tomography (SD-OCT) and mesopic fundus-guided microperimetry (MP).[12,13] OCT provides non-invasive visualization and allows objective quantification of retinal structure in patients with IRD.[14–16] While these measurements correlate with visual function measures, ellipsoid zone (EZ) band width and area have higher reliability than functional measures such as visual acuity (VA), visual field, and electroretinogram responses.[14,17] Prior studies have not investigated the association of EZ measures with visual function in patients with *USH2A*-associated IRD. Fundus-guided MP, which provides a topographic evaluation of retinal function across the macula with greater precision and resolution than standard perimetry, can also be correlated with OCT measures of macular retinal structure.[18–20]

As new treatments for *USH2A*-related IRD are being evaluated,[21,22] an accurate knowledge of the natural history of *USH2A*-associated IRD is essential to best identify outcome measures suitable for clinical studies of therapies. This multicenter, international, longitudinal study of participants with retinal degeneration associated with *USH2A* sequence variants, the Rate of Progression of *USH2A*-related Retinal Degeneration (RUSH2A) study, was designed with the primary objective to characterize the natural history of *USH2A*-related retinal degeneration over 4 years. The study employs functional, structural, and patient-reported outcome measures to characterize variability in endpoints and possible risk factors (genotype, phenotype, and comorbidities) for disease progression.

The main objective herein is to address the unmet need stemming from the paucity of robust, quantitative structural and functional outcome measures characterizing retinal degeneration related to *USH2A* variants. We report RUSH2A baseline data on OCT and mesopic

MP in participants with *USH2A*-related USH2 compared to *USH2A*-related ARRP and explore macular structure-function associations and relationships with baseline participant characteristics.

Materials and Methods

Study Design

Participants were enrolled in the RUSH2A study (NCT03146078) at 16 clinical sites in Europe and North America. The study was approved by the ethics boards at each site and adhered to the tenets of the Declaration of Helsinki. The study design and inclusion and exclusion criteria were previously documented.[12] Briefly, study participants were at least 8 years of age with a clinical diagnosis of rod-cone degeneration associated with at least 2 pathogenic or likely pathogenic sequence variants in *USH2A*. Following informed consent and initial eligibility assessment and informed consent, some individuals without a history of hearing loss and presumed nonsyndromic ARRP underwent additional genetic testing of first-degree relatives to confirm *in trans* inheritance of the variants. After enrollment, an independent audiologist reviewed the history of hearing loss and the results of baseline audiology exams to confirm either the USH2 or the ARRP diagnosis. Disease duration was computed based on age of onset, date of awareness of visual symptoms on participant medical history forms, and date of study enrollment.

Participants with a baseline best corrected visual acuity (BCVA) with Early Treatment of Diabetic Retinopathy Study (ETDRS)[23] letter score of 54 or greater (Snellen equivalent 20/80 or better) in the study eye, kinetic visual field at least 10° diameter in all meridians using the III4e target (Octopus 900 Pro, Haag Streit, Mason, Ohio), and stable fixation were enrolled in the primary cohort with a target sample size of 100. The study was also designed to enroll a secondary cohort of 20 participants with study eye baseline ETDRS letter score of 53 or less (Snellen equivalent 20/100 or worse), central visual field of less than 108 diameter, or unstable fixation. Secondary cohort was designed to complete a baseline visit only. The study eye was defined as the eye with better VA at baseline.

The schedule of assessments and testing procedures for this natural history study have been described previously.[12] This prior report provides details of other measures evaluated for correlation with MP and OCT measures of interest, including BCVA determined by ETDRS letter score and static perimetry total hill of vision (V_{TOT}). All MP and OCT testing was performed by technicians certified by the Duke Reading Center respecting the study-specific protocol and standardized procedures. Fundus-guided mesopic (standard) MP was performed using a Macular Integrity Assessment (MAIA-2) unit (iCare, Raleigh, NC) with software version 1.7 or higher. Sites performed baseline MP in the study eye, in primary cohort participants only. The test was performed three times to evaluate test-retest repeatability and to mitigate a potential learning effect. Two sites did not have the equipment and therefore MP was not performed in the participants from these sites. OCT volume scans were obtained using a Heidelberg Spectralis HRA+OCT unit (Heidelberg Engineering GmbH, Heidelberg, Germany). Sites performed baseline OCT in both eyes of all participants. The OCT and MP measures reported herein are mean retinal sensitivity from

MP; and intact EZ area, central 1 mm subfield thickness (CST), presence of intraretinal cysts, epiretinal membrane (ERM) or vitreomacular traction (VMT) from OCT.

Microperimetry Imaging and Grading

MP testing was administered following pupillary dilation with one drop of tropicamide 1% and phenylephrine 2.5%. Participants were in a mesopic environment for at least 10 min prior to testing and completed a two-minute training session prior to the full test. The full test involved a custom, circular grid consisting of 89 points that covered the macular area and to the arcades. The custom grid was composed of 89 stimuli arranged in concentric crowns located at 2°,4°, 6.5°, 9°, 12° and 15° from the foveal center.

Readers at the Duke Reading Center evaluated all MP images. A retinal sensitivity of <25 dB was considered abnormal, and sensitivity of <0 dB was considered to represent an absolute scotoma. The foveal area was determined based on the red-free fundus image[24] by use of the perimacular vessels and the center of the avascular zone. Eyes with abnormal sensitivity <25 dB in the foveal area were classified as having foveal involvement. Fixation stability was expressed as the bivariate contour ellipse area (BCEA), the area of an ellipse on the retinal surface within which the center of the target was imaged at least 68% of the time; smaller values indicate more precise fixation.[25]

OCT Imaging and Grading

High resolution, macula-centered, spectral domain OCT volume scans consisting of 121 B-scans within a 30° × 25° retinal area using automatic real-time (ART) tracking setting of 9, and one 7-line raster scan with a 30° × 5° area at ART 25 were acquired.

Duke Reading Center readers assessed all OCT scans; grayscale was used for additional contrast. The presence or absence of retinal cystic changes were determined within the retinal layers, not between ERM and the retina or associated with choroidal neovascularization, pigment epithelial detachment, or other area outside the neurosensory retinal tissue. Retinal cystic changes were considered well-defined, black or dark round or oval shapes, and were differentiated from diffuse edema characterized by absence of well-defined round or oval shapes, and from outer retinal tubulations.

ERM and VMT deformation within 1 mm of the foveal center were defined as whether the presence of ERM or posterior hyaloid, respectively, deformed the retina within this area. CST was measured semi-automatically by the HEYEX software version 6.12 (Heidelberg Engineering GmBH, Heidelberg, Germany). Readers first adjusted image centration, and then corrected inner and outer segmentation boundaries (the internal limiting membrane and Bruch's membrane) as needed.

The Duke Optical Coherence Tomography Retinal Analysis Program (DOCTRAP)[26,27] was used to manually annotate A-scans with intact EZ on each B-scan from OCT macular volumes and to calculate intact EZ area. Readers first annotated the foveal B-scan on which the intact EZ is easier to identify, and then annotated the neighboring B-scans. In borderline cases where the presence or absence of the EZ was not clear, the reader assumed EZ

continuity from the fovea. A second senior reader reviewed all B-scan gradings of the first reader and corrected the gradings when needed.

Microperimetry-OCT Overlays

To overlay the MP microperimetry sensitivity grid and intact EZ area segmented on the OCT images, a semi-automated software program was developed to register the infrared (IR) fundus image acquired during OCT imaging to the microperimetry fundus image. As the images were simultaneously acquired, the intact EZ area could also be mapped onto the IR image. A reader identified and selected pairs of corresponding points at various locations on the IR image and microperimetry image, usually at prominent vessel bifurcations or crossings and over as wide an area as possible. The software then estimated the subcategories of the geometric transformation (affine, similarity, or projection) by mapping the pairs of corresponding points between the images. To estimate the transformation parameters, the reader identified a minimum of four pairs of corresponding points in these images. In most cases, affine transform (which encompasses scaling, rotation, shear, and translation) was found to be the best model for mapping the IR image and microperimetry images. The accuracy of the estimated geometric transformation was determined by the complete vessel overlap between the images. A second reader reviewed the registered images and identified and selected additional pairs of corresponding points to improve the registration where necessary and possible. Figure 1 (A–E) shows an example of the MP-OCT overlay.

Once the images were successfully registered, the aggregate and average retinal sensitivities were calculated, inside and outside the intact EZ area, respectively. Any locus with retinal sensitivity <0 dB was assigned a value of −1 dB. The aggregate retinal sensitivity was calculated by summing the retinal sensitivity for each locus inside and outside the intact EZ area, respectively, including the −1 values. The average retinal sensitivity was calculated by dividing the aggregate retinal sensitivity by the number of loci inside and outside the intact EZ area, respectively.

Additionally, as the resolution of the IR image was higher than the density of loci on the MP grid map, the MP map was interpolated using natural neighbor interpolation[28] to achieve similar pixel density to the IR image. The interpolated microperimetry map was thresholded to a minimum value of −1 dB and maximum value of 36 dB, according to the MAIA range of values. The aggregate interpolated retinal sensitivity was calculated by summing the interpolated retinal sensitivity inside and outside the intact EZ area, respectively. The average interpolated retinal sensitivity was calculated by dividing the aggregate interpolated retinal sensitivity by the number of pixels inside and outside the intact EZ area, respectively. This method, which includes the loci with absolute scotoma (0 dB not seen) in the measures of average sensitivities, is different from the total hill of vision methodology[12,29] which excludes retinal areas in which the light stimulus is not seen.

Statistical Methods

The distributions of baseline characteristics and measures of visual function and structure for the whole study cohort were previously detailed in Duncan et al.[12] The within-visit

variation in the 3 MP tests performed at baseline was evaluated using intra-class correlation coefficients (ICC). In addition, the repeatability coefficient and Bland-Altman plots[30] were used to assess variability of repeated MP tests. The average of the first and second mean sensitivity of MP tests for each of the participants was used for analyses of the mean sensitivity (average threshold). Average point-wise sensitivity between repeated tests was determined using a linear mixed effects model, considering test sequence number as a fixed effect and points within eye as a random effect.[31] General linear models were employed to assess the association of baseline characteristics with mean retinal sensitivity of MP and OCT EZ area. Since the course of disease could be different between USH2 and ARRP participants, clinical diagnosis was adjusted in the model regardless of statistical significance. Significant factors retained in the final model were adjusted in following analysis. The square root transformation was used for skewed outcome distributions in regression models. The associations between baseline mean retinal sensitivity of MP and OCT EZ area with other functional and structural measures were evaluated by calculating Spearman correlation coefficients. Unreliable MP test results (fixation losses ≥30%) and ungradable OCT scans were excluded from all analysis.

Symmetry of the EZ area between left and right eyes was assessed using scatterplots and summarized with ICCs. The magnitudes of differences and their association with the area size were assessed using Bland-Altman plots.

Missing data were treated as a separate category for discrete factors, and a missing indicator was created for continuous factors. Continuous covariates were included in all models in continuous form but were categorized for display and ease of interpretation in the tables. All reported *P*-values were 2-sided. Due to the descriptive and exploratory nature of this analysis, the P-values were not adjusted for multiple comparisons. Statistical analyses were conducted using SAS software version 9.4 (SAS, Inc) and the R system (v. 3.5.1).

Results

Study Population

One hundred and five (83%) of the 127 subjects recruited in the RUSH2A study were included in the primary cohort, and 22 (17%) in the secondary cohort. The OCT from one eye was ungradable as the EZ extended beyond the scan area. Of the 95 participants in the primary cohort with MP testing, 93 test 1, 92 test 2, and 91 test 3 were completed. Incorrect MP grids were submitted for 3 participants and 3 were submitted with an incorrect projection strategy. Three test 2 and 5 test 3 MP results were excluded due to fixation losses > 30% (denoting an unreliable exam). Eighty seven test 1, 83 test 2 and 80 test 3 MP results were included in the analysis.

Key baseline characteristics of all participants were detailed in a previous RUSH2A manuscript.[12] Summary statistics for the MP analysis cohort are provided in Table 1 and stratified by clinical diagnosis (52 [60%] USH2 and 35 [40%] ARRP). Forty-eight (55%) participants were female and 79 (91%) were white. The median (interquartile range [IQR]) age was 34 (26, 42) years in the USH2 group and 38 (35, 48) years in the ARRP group.

Variability of Microperimetry Testing

The median (IQR) of the mean sensitivity on test 1, 2, and 3 was 4.3 (2.5, 8.7), 3.8 (2.4, 8.5), and 3.6 (2.1, 6.8) dB, respectively. No learning effect was identified, as test 1 had a slightly higher mean sensitivity denoting better performance than the following tests, and perhaps indicating fatigue with repeated test sessions. Bland-Altman plots showed mean differences near 0 with 95% limits of agreement of ± 2.0 dB (Figure 2). Participants with different BCVA or amount of experience on MP test due to disease duration had similar repeatability (data not shown).

Although the overall repeatability of mean sensitivity for 78 participants with 3 available measures was high (ICC=0.97 with 95% CI (0.97,0.99), repeatability coefficient = 2.2), the third test had the lowest average value and differed from the average value of test 1 (4.3 vs 3.6, $P = 0.004$). A sub-analysis of loci with non-zero sensitivity yielded similar results (ICC 0.96 with 95% CI [0.95, 0.97], repeatability coefficient 2.5). The third MP test still had the lowest average value (test 1 vs test 3: 14.0 dB vs 13.6 dB, P=0.05). Based on the possibility of participant fatigue during the third test, it was eliminated from subsequent MP analyses, and the mean retinal sensitivity was subsequently analyzed using the average of the first and second tests.

Point-wise sensitivity for each test was tabulated and stratified by eccentricity from the foveal center (e-Table 1). Foveal sensitivity was similar to the surrounding loci, as previously observed .[32,33] The central MP loci had better sensitivity than peripheral loci (Figure 3). Foveal involvement was defined as retinal sensitivity of < 25 dB in the foveal area. The overall point-wise coefficient of repeatability was 8.9 dB, and decreased to 8.1 dB when the analysis excluded points with absolute scotoma (sensitivity <0 dB) (e-Table 2).

Microperimetry Metrics

Microperimetry measures at baseline are summarized in Table 2. The median (IQR) sensitivity was 3.5 (2.1, 8.4) dB in USH2 participants, and 5.1 (2.9, 9.0) dB in ARRP participants (P=0.13). The median (IQR) 95% BCEA area was similar by clinical diagnosis (1.3 (0.8, 2.8) vs 1.7 (0.8, 2.8); P=0.83). The median (IQR) number of loci with abnormal sensitivity (<25 dB) was comparable by clinical diagnosis (88 (85, 89) vs 86 (81, 88); P= 0.23). Forty-eight (92%) participants in the USH2 group and 25 (71%) in ARRP, respectively, had foveal involvement on at least one test. Foveal involvement was not associated with clinical diagnosis (P=0.06) or disease duration (P=0.14). One participant in the USH2 group had unstable fixation on all tests. All ARRP participants had stable fixation on at least one test.

Mean sensitivity values stratified by baseline participant characteristics are shown in Table 3. Clinical diagnosis was not statistically significantly associated with mean sensitivity (P=0.55). Among all participants and within each diagnosis group, mean sensitivity decreased with increasing duration of disease (P-value=0.01; mean decrease of 0.13 with 95% CI (0.3, 0.56) dB for each additional year of duration). No other baseline characteristic in Table 3 was found to be significantly associated with mean sensitivity.

The association of other baseline functional and structural measures with mean sensitivity are summarized in Table 4. Better BCVA was associated with higher mean sensitivity values (Spearman correlation coefficient r=0.34 with 95% CI 0.13 to 0.51). Larger EZ area and larger CST were associated with a greater mean sensitivity (r=0.68, with 95% CI 0.55 to 0.78 and r=0.37, with 95% CI 0.17 to 0.54, respectively).

OCT Features

Baseline OCT features are summarized in Table 5. 55% (70 of 127) participants had no cysts present at baseline. One participant with USH2 had VMT with deformation within the central 1 mm. Twenty-five (20%) participants had ERM with deformation within the central 1 mm, 13 (16%) in the USH2 group and 12 (26%) in the ARRP group (P=0.25). VA was not associated with ERM (P=0.69). The central structural measures of intact EZ area (median (IQR) 1.4 (0.4, 3.1) mm^2 vs 2.3 (0.7, 5.7) mm^2, P=0.12, 95% CI of difference in median −1.74 to 0.38) and CST (247 (223, 280) μm vs 261 (246, 288) μm, p=0.17, 95% CI of difference in median −30.52 to 2.52) were similar between USH2 and ARRP participants.

The association of baseline participant characteristics with intraretinal cysts is summarized in Table 6. The distribution of presence and location of cysts was similar in both clinical diagnosis groups (P=0.22). Participants without cysts had lower CST compared with participants with cysts (252 (226, 279) μm vs 261 (232, 288) μm, P<0.001). In addition, absence of cysts was associated with greater BCVA (83 (75, 87) vs 77 (72, 83), P=0.01).

Intact EZ area stratified by baseline participant characteristics is shown in Table 7. Clinical diagnosis was not statistically significantly associated with EZ area (P=0.75). Longer duration of disease was associated with smaller EZ area (P<0.001; mean decrease of 0.16 with 95% CI (0.8, 0.25) mm^2 for each additional year of duration).

The association of other baseline functional and structural measures with mean sensitivity are summarized in Table 8. Better BCVA (r=0.61 with 95% CI 0.48 to 0.71) and greater CST (r= 0.67 with 95% CI 0.57 to 0.76) were associated with greater EZ area. Intact EZ area was similar for participants regardless of spherical equivalent (r=−0.13 with 95% CI −0.31 to 0.05).

MP-OCT Correlation

MP-OCT overlay data stratified by clinical diagnosis and disease duration are provided in Table 9. The median (IQR) average sensitivity within intact EZ was 23 (21, 25) dB, and decreased to 21 (19, 24) dB when interpolated. The median (IQR) average sensitivity outside the intact EZ area was 2 (1, 6) dB and remain similar when interpolated. Average sensitivities (with and without interpolation) within the intact EZ area and outside the intact EZ area were similar by clinical diagnosis. The interpolated average sensitivity within the intact EZ area and outside intact EZ area both decreased with disease duration.

Participants in the USH2 group and with longer disease duration had a smaller number of pixels and sensitivity points within the intact EZ area, but more sensitivity points outside the intact EZ area (Table 9). Overall, the ratio of interpolated average sensitivity inside the intact

EZ to outside the intact EZ was 8, and the ratio was not statistically significantly associated with clinical diagnosis or disease duration.

Interocular Variability and Symmetry of OCT EZ area

Median (IQR) EZ area for left and right eyes was 1.5 (0.4, 3.6) and 1.6 (0.6, 3.9) mm^2, respectively, demonstrating a high concordance (ICC=0.96 with 95%CI (0.94, 0.97)) between the two eyes. Bland-Altman plots (Figure 4) showed a mean difference (left minus right) between eyes equal to -0.02 mm^2 with limits of agreement ± 3.2 mm^2 (about 2.4%).

Genetic Analysis

Following our findings in the RUSH2A genetics study[34] we investigated whether genetic variants in *USH2A* correlate with OCT and MP findings. While there was no difference in the presence or absence of macular cysts between clinical diagnosis subgroups, the presence of cysts correlated with the number of truncating alleles across the entire cohort (29 patients; $P = 0.03$) and in the ARRP group (35 patients; $P = 0.05$) on logistic regression analysis (Figure 5A–B). However, we did not find any significant associations between truncating allele number and presence of macular cysts in the USH2 group when analyzed separately (data not shown).

Similar to our previous report that certain *USH2A* missense variants are hypomporphic, when comparing patients with ARRP-associate missense alleles p.Cys759Phe, p.Cys3294Trp, and p.Cys3358Tyr to those with other missense alleles, the mean sensitivity outside the intact EZ was increased in ARRP (Figure 6). There were no differences in intact EZ area or retinal sensitivity on MP when comparing these groups.

Discussion

In this work, we report baseline data on OCT and mesopic MP in *USH2A*-related USH2 as compared to nonsyndromic ARRP and the relationships with baseline patient characteristics in the multicenter, international RUSH2A natural history study. We showed that participants with USH2 and ARRP had comparable EZ area and mean sensitivity on MP testing. Longer disease duration correlated with more severe macular abnormalities, specifically smaller intact EZ area and lower mean sensitivity on MP testing. Better BCVA, and larger CST were associated with larger EZ area, and all metrics positively correlated with retinal sensitivity.

The relevant outcome measures analyzed in this study were mean retinal sensitivity on MP, EZ area, CST, and presence of intraretinal cysts or CME, ERM, and VMT on OCT. Three separate MP tests were employed to investigate the presence of a learning effect in this specific patient population. We found that no learning effect was identified, regardless of baseline BCVA characteristics or disease duration. These results are similar to those obtained with MP testing in early AMD and type 2 macular telangiectasia, in which most studies failed to report improvements in MP metrics during the second visit,[35–37] while others noted the presence of a learning effect influencing mean sensitivity.[31,38] The discrepancy between the studies may be due to the different testing parameters used, statistical analyses applied, and use of a training exam. Before performing the baseline MP test, all RUSH 2A participants underwent a brief 2 min training exam, which may

have contributed to the absence of a learning effect during test 1. Instead of a learning effect, MP mean sensitivity was highest on test 1, and lowest on test 3. As test 2 and 3 had a similarstarting dB as for test 1, and a 4-2 staircase algorithm was employed for all exams, the testing protocol would not be expected to yield lower mean sensitivities for test 3. In addition, MAIA microperimetry has high test-retest repeatability using the follow-up function.[39] In our study, the proportion of subjects with unreliable tests (fixation losses > 30%) was highest during the last test. As all baseline tests were performed on the same day, the decreased sensitivity and increase in unreliable tests could potentially be attributed to patient fatigue during the last test. The loss of mean sensitivity due to patient fatigue has been previously described in automated perimetry testing.[40] Sabates and colleagues showed that fatigue also decreased retinal sensitivity on microperimetry testing in healthy subjects, as subjects that had only a short resting period between testing sessions were more likely to show a decrease in retinal sensitivity between the first and second eye tested (Sabates FN et al., written communication, April 2009). This finding is informative for future clinical trials of inherited retinal degeneration in which MP is used, in which it is recommended that baseline MP assessments are done on separate days. Our results also suggest that the first MP test or an average of the first two should serve as the baseline measurement, in contrast with other prior clinical trials in which the third MP test or a later test was used as the baseline.[41,42]

The topographic assessment afforded by MP testing in this study revealed that central retinal loci among participants with USH2 and ARRP patients had better sensitivity than the peripheral loci, consistent with the centripetal nature of these conditions. This trend is similar to data obtained with the Nidek MP-1[43,44], Nidek MP-3[45] and the MAIA device in patients with RP.[41]

Median sensitivity was slightly lower in participants with USH2 than those with ARRP but this trend did not reach statistical significance, similar to the findings on static perimetry in the RUSH2A baseline visit,[12] in which V_{30} was similar regardless of diagnosis. The mean and median sensitivity values were overall low and the fovea was involved in the majority of participants (66%), despite stable fixation in 93% of participants. The only significant associations with higher mean sensitivity across the macula were better BCVA, shorter disease duration, larger EZ area and greater CST.

Charng and colleagues recently analyzed MAIA MP cross-sectionally and longitudinally in a cohort of 16 patients with USH2A-related retinal degeneration.[46] Using a grid with a diameter of 18°, they noted a mean sensitivity of 10.0 dB. The higher mean sensitivity value than that shown in our study was expected given the smaller grid used in that trial compared to the 30°diameter pattern employed in the RUSH2A study. The authors also demonstrated that sensitivity at the edge of the scotoma had the fastest rate of functional decline over an average of 2.6 years compared to mean sensitivity and responding point sensitivity,[46] suggesting that the edge of scotoma sensitivity would be a useful metric for longitudinal analysis in the RUSH2A study.

On OCT, we noted that CST and EZ area were similar between the USH2 and ARRP groups. Greater intact OCT EZ area was associated with shorter disease duration, better

BCVA, and larger CST, all variables denoting earlier disease stages. In the overall cohort, the presence of intraretinal cysts was associated with worse BCVA. Interestingly, the presence of intraretinal cysts correlated with the number of truncating alleles across the entire cohort and in the nonsyndromic ARRP group.

On MP-OCT overlay analysis, there were no differences in average retinal sensitivity with or without interpolation between the USH2 and ARRP groups. Our results contrast with a European study in which participants with USH2 had more severe symptoms and earlier visual acuity and visual field loss than ARRP.[11] However, this study did not use high-resolution OCT or MP technology to investigate structural and functional loss, and did not control for disease duration in the analyses of symptom severity and visual loss. In RUSH2A, the interpolated average sensitivity within intact EZ area and number of non-scotomatous points (≥ 0 dB) decreased with disease duration, suggesting that the loss of function with worsening disease preceded the structural change of EZ loss. We found a high ratio between sensitivity within intact EZ to sensitivity outside intact EZ, consistent with the fairly abrupt change in sensitivity across transition zone shown by Hood et al.[15], Birch et al.[16] and Rangaswamy et al.[47]

Our analysis of the structure-function correlation was characterized by specific methodologic differences from prior studies. The method of computing aggregate retinal sensitivity differed from that used in relevant previous publications for analysis of EZ area-MP overlays in macular telangiectasia type 2 (MacTel).[20,48] The aggregate retinal sensitivity loss in MacTel used the sum of the absolute difference of the retinal sensitivities of the EZ defect (i.e. region outside the intact EZ area) relative to the background sensitivity (i.e. average retinal sensitivity inside the intact EZ area) to describe the EZ defect area and scotoma depth in a single variable. However, it was determined to be unsuitable in this study, as the EZ defect in RUSH2A subjects extended beyond the imaging field of view, so that it was not feasible to determine a true background sensitivity. In RUSH2A, the infrared image was used for registration instead of the summed voxel projection (SVP) image used in the MacTel analysis,[20] as the infrared image has a larger field of view and provides superior visualization of the anatomical features useful for registration compared to the SVP image. In addition, the generation of the SVP image requires segmentation of both the inner and outer EZ layer boundaries, whereas the EZ layer segmentation in the RUSH2A study used only a single line to indicate the presence of intact EZ.

Previous studies have linked deleterious loss-of-function alleles (nonsense, frameshift, splice-altering) to USH2 severity, including hearing loss.[11,49] We found that truncating allele number and not clinical diagnosis were associated with the presence of macular cysts, particularly in patients with two truncating alleles. Although we did not observe a decrease in the intact EZ area size or sensitivity in patients with biallelic loss-of-function mutations, this finding suggested that patients with biallelic loss-of-function variants may have a higher biological predisposition for cyst formation. Further, a subset of missense alleles was enriched in patients without hearing loss[50] (R.B. Hufnagel, MD, PhD, unpublished data, November 2021). Recently, we expanded on these findings to demonstrate that these missense alleles are associated with later age of vision loss onset and improved field of vision and electrophysiological responses (R.B. Hufnagel, MD, PhD, unpublished data,

November 2021). Here, we found that, while the intact EZ zone itself is not affected, both average and aggregate sensitivity in degenerating retina outside this region are increased in patients harboring these missense alleles compared to patients with other *USH2A* variants. These data add further evidence to the concept that these missense variants are associated with slower progression of disease and warrant closer inspection in natural history studies and when defining outcome measures for clinical treatment trials.

The current study had several limitations. The study was a baseline exploratory analysis in which no adjustments were made to control for multiple comparisons. As with other papers in this field, we report the lateral OCT measurements (e.g., scan length, EZ area, and EZ bandwidth) in millimeters. The accuracy of these values depends on the accuracy of the pixel-to-micron conversion factor [51] provided by the manufacturer, which could vary between patients or even within a patient over time. It is important to note that any inaccuracies in scaling may impact the intermodality correlative analyses and the intramodality longitudinal analyses to varying degrees. Lastly, only patients with a baseline BCVA with ETDRS letter score of 54 or greater (Snellen equivalent 20/80 or better) in the study eye were enrolled in the RUSH2A study, therefore the findings described cannot be necessarily extrapolated to patients with worse BCVA.

The strengths were the large sample size of participants with *USH2A*-related retinal degeneration, especially given the relative rarity of the diseases studied, the use of standard study protocols using new technology to acquire data (OCT, mesopic MAIA MP), and software specifically developed for analyzing the correlation between function and structure through en face OCT-MP overlays. In addition, a learning effect and test-retest variability were carefully addressed as critical factors in a psychophysical test such as MP and showed that repeated testing increased variability, and that specific genetic variants correlated with phenotypic manifestations of disease severity.

The data obtained in the baseline visit of the RUSH2A study, especially the information on test-retest repeatability and intervisit variability, have key implications in the design of future therapeutic clinical studies of *USH2A*-related retinal degeneration. The genotype-phenotype correlations will also provide valuable information to guide consideration of the best patient populations to include in early phase trials that evaluate a treatment effect. Given the strong structure-function associations identified between BCVA, EZ area and CST on OCT images, this work demonstrates that OCT and MP are outcome measures that should be included in interventional studies. Next steps will involve identification of individuals that would progress to loss of visual function based on OCT alone, which would potentially allow objective structural endpoints to become primary outcome measures in future studies of *USH2A*-related retinal degeneration.

Supplementary Material

Refer to Web version on PubMed Central for supplementary material.

Funding/Support:

Funded by Foundation Fighting Blindness.

Financial Disclosures:

E.M. Lad receives grants or contracts from Novartis, consulting fees Iveric Bio; **J.L. Duncan** receives grants awarded to UCSF from the National Eye Insitute, Foundatin Fighting Blindness, L.L. Hillblom Foundation, Biogen/Nightstarx for Xolaris natural history study, Abbvie/Allergan for RST-001 study, Acucela Inc. for SeaStar Study, and Neurotech Inc for monitoring and material support for NT-501 study, she also receives consulting fees from DTx Therapeutics, Conesight, Eloxx, Eyevensys, Editas, Helios, PYC Therapautics, ProQR, Vedere Bio II, Gyroscope (SAB), Nacuity (SAB), SparingVision and she serves on a monitoring or advisory board for AGTC Therapeutics (DSMC membership), ProQR (DSMC member), Spark Therapeutics (DSMC member), and serves in a leadership role as chair, scientific advisory board, Foundation Fighting Blindness; **M.G.Maguire** receives support from Foundation Fighting Blindness, grants or contracts from National Eye Institute; **I. Audo; D.G. Birch** receives grants or contracts from NIH-EY009076, receives payment or honoraria from AGTC, Nacuity Pharmaceuticals, ProQR, Editas, 4D Molecular Therapeutics, Novartis, participates on data safety monitoring or advisory board for ReNeuron, and serves on a SAB for Foundation Fighting Blindness**; J. Carroll** receives research funding to institution from Foundation Fighting Blindness, receives royalties or licenses from Translational Imaging Innovations-Equity Interest, Consulting fees for AGTC, Meira GTx, Optovue**; J.K. Cheetham** receives personal payments from Foundation Fighting Blindness, consulting fees from DTx Pharma Therapeutics, and has stock or stock options with AbbVie**; T.A. Durham** receives consulting fees from Novartis**; A.T. Fahim** receives grants or contracts from National Eye Institute (K12EY022299), Research to Prevent Blindness, Choroiderma Research Foundation, and Eversight, Participates on an advisory board for Foundation Fighting Blindness, and has stock with Ionis Pharmaceuticals; **E. Heon** receives support from Henry Brent Chair for innovative pediatric ophthalmology research; **A. Iannaccone** receives support for the present manuscript from Foundation Fighting Blindness and Research to Prevent Blindness, Inc Unrestricted grant to Duke Eye Center, receives grants or contracts from 4D Molecular Therapeutics, Acucela, AGTC, Royalties or licenses from Springer, consulting fees from Allievex, Guidepoint, Arkin Holdings, Gyroscope/Novartis, Atheneum Partners, IQVIA, Baker Brothers, Janssen, ClearView Healthcare Partners, Kairos Ventures, Endogena, Rhythm Pharmaceuticals, GLG Group, Teladoc Health, particpatres on a data safety monitoring board for Alia Therapeutics, Janssen, and is in a leadership or fiduciary role for Blue Cone Monochromacy Families Foundation (SAB), Choroideremia Research Foundation (SAB), Foundation Fighting Blindness (SAB);**C.N. Kay** receives consulting fees from AGTC, Spark Therapeutics, Novartis, Astena Therapeutics, Lexitas, Kiora, she receives payment or honoraria from Spark Therapeutics, and grant support from AGTC, FFB, Alekus, Gyroscope, Regenx Bio, Nightstarx Therapeutics/ Biogen, Iveric Biom ProQR Therapeutics, Meira GTx/Janssen, Kodiak, 4D Therapeutics, and has Astena Therapeutics stock**; M.E. Pennesi** receives consulting fees from 4D Molecular Therapetuics, Abbvie, Adverum, AGTC, Ascidian, Astellas Pharmaceuticals, Atsena, Bayer, Biogen, Blue Rock, Chlogene, DTx Therapeutics, Editas, Endogena, Eyevensys, Horama, IVERIC, Janssen, Nacuity Pharmaceuticals, Novartis, Ocugen, Ora, ProQR, PYC Therapeutics, RegenexBio, Roche, Sanofi, Saliogen, Sparing Vision, Viewpoint Therapeutics, Vedere; and participates on a data safety monitoring board or advisory board for Akous, and Gensight, and other non-financial interests with FFB for clinical trial support; **C.Y. Weng** receives consulting fees from Allergan/Abbive, Alcon, Alimera Sciences, DORC, Regeneron, REGENXBIO, Genentech, Novartis and is a board member for American Society of Retina Specialists, American Scoiety of Cataract and Refractive Surgery and Woman in Ophthalmology**; S. Farsiu** receives support for the present work from FFB, NIH/NEI (P30-EY005722), and an unrestricted grant from research to Prevent Blindness to Duke Eye Center and patents issued US patents 8,811,745, and 9,299,155, and 9,589,346, and 9,940,722, and **W. Liang, A.R. Ayala, J. Loo, Z. Deng; D. Mukherjee, M. Michaelides, R.B. Hufnagel, B. Guan, G. J. Jaffe**, **A. Vincent** report none

Other Acknowledgments:

Michel Michaelidesis supported by a grant from the National Institute for Health Research Biomedical Research Centre at Moorfields Eye Hospital NHS Foundation Trust and UCL Institute of Ophthalmology. AV is supported by Foundation Fighting Blindness, USA (**CD-CL-0617-0727-HSC).** EH holds the Henry Brent Chair in innovative Pediatric Ophthalmology research. JLD serves on advisory boards for the Foundation Fighting Blindness and is supported, in part, by the UCSF Vision Core shared resource of the NIH/NEI P30 EY002162, and by an unrestricted grant from Research to Prevent Blindness, New York, NY. Dr. Pennesi serves on advisory boards for Foundation Fighting Blindness. This relationship has been reviewed and NEI P30 EY002162 - Core Grant for Vision Research, managed by OHSU. Dr. Birch is supported by NEI 09076. SF is supported, in part, by the NIH/NEI P30-EY005722, and by an unrestricted grant from Research to Prevent Blindness to Duke Eye Center.

References

1. Ferrari S, Di Iorio E, Barbaro V, Ponzin D, Sorrentino FS, Parmeggiani F. Retinitis pigmentosa: genes and disease mechanisms. Curr Genomics. 2011;12(4):238–249. [PubMed: 22131869]
2. Mathur P, Yang J. Usher syndrome: Hearing loss, retinal degeneration and associated abnormalities. Biochim Biophys Acta. 2015;1852(3):406–420. [PubMed: 25481835]

3. Eudy JD, Weston MD, Yao S, et al. Mutation of a gene encoding a protein with extracellular matrix motifs in Usher syndrome type IIa. Science. 1998;280(5370):1753–1757. [PubMed: 9624053]
4. Fishman GA, Kumar A, Joseph ME, Torok N, Anderson RJ. Usher's syndrome Ophthalmic and neuro-otologic findings suggesting genetic heterogeneity. Arch Ophthalmol. 1983;101(9):1367–1374. [PubMed: 6604514]
5. McGee TL, Seyedahmadi BJ, Sweeney MO, Dryja TP, Berson EL. Novel mutations in the long isoform of the USH2A gene in patients with Usher syndrome type II or non-syndromic retinitis pigmentosa. J Med Genet. 2010;47(7):499–506. [PubMed: 20507924]
6. Le Quesne Stabej P, Saihan Z, Rangesh N, et al. Comprehensive sequence analysis of nine Usher syndrome genes in the UK National Collaborative Usher Study. J Med Genet. 2012;49(1):27–36. [PubMed: 22135276]
7. Jacobson SG, Cideciyan AV, Aleman TS, et al. Usher syndromes due to MYO7A, PCDH15, USH2A or GPR98 mutations share retinal disease mechanism. Hum Mol Genet. 2008;17(15):2405–2415. [PubMed: 18463160]
8. Schwartz SB, Aleman TS, Cideciyan AV, et al. Disease expression in Usher syndrome caused by VLGR1 gene mutation (USH2C) and comparison with USH2A phenotype. Invest Ophthalmol Vis Sci. 2005;46(2):734–743. [PubMed: 15671307]
9. Iannaccone A, Kritchevsky SB, Ciccarelli ML, et al. Kinetics of Visual Field Loss in Usher Syndrome Type II. Invest Ophthalmol Vis Sci. 2004;45(3):784–792. [PubMed: 14985291]
10. Fishman GA, Bozbeyoglu S, Massof RW, Kimberling W. Natural course of visual field loss in patients with Type 2 Usher syndrome. Retina. 2007;27(5):601–608. [PubMed: 17558323]
11. Pierrache LH, Hartel BP, van Wijk E, et al. Visual Prognosis in USH2A-Associated Retinitis Pigmentosa Is Worse for Patients with Usher Syndrome Type IIa Than for Those with Nonsyndromic Retinitis Pigmentosa. Ophthalmology. 2016;123(5):1151–1160. [PubMed: 26927203]
12. Duncan JL, Liang W, Maguire MG, et al. Baseline Visual Field Findings in the RUSH2A Study: Associated Factors and Correlation with Other Measures of Disease Severity. Am J Ophthalmol. 2020;219:87–100. [PubMed: 32446738]
13. Birch DG, Cheng P, Duncan JL, et al. The RUSH2A Study: Best-Corrected Visual Acuity, Full-Field Electroretinography Amplitudes, and Full-Field Stimulus Thresholds at Baseline. Transl Vis Sci Technol. 2020;9(11):9–9.
14. Birch DG, Locke KG, Wen Y, Locke KI, Hoffman DR, Hood DC. Spectral-domain optical coherence tomography measures of outer segment layer progression in patients with X-linked retinitis pigmentosa. JAMA Ophthalmol. 2013;131(9):1143–1150. [PubMed: 23828615]
15. Hood DC, Ramachandran R, Holopigian K, Lazow M, Birch DG, Greenstein VC. Method for deriving visual field boundaries from OCT scans of patients with retinitis pigmentosa. Biomed Opt Express. 2011;2(5):1106–1114. [PubMed: 21559123]
16. Birch DG, Locke KG, Felius J, et al. Rates of decline in regions of the visual field defined by frequency-domain optical coherence tomography in patients with RPGR-mediated X-linked retinitis pigmentosa. Ophthalmology. 2015;122(4):833–839. [PubMed: 25556114]
17. Hariri AH, Zhang HY, Ho A, et al. Quantification of Ellipsoid Zone Changes in Retinitis Pigmentosa Using en Face Spectral Domain–Optical Coherence Tomography. JAMA Ophthalmol. 2016;134(6):628–635. [PubMed: 27031504]
18. Birch DG, Wen Y, Locke K, Hood DC. Rod sensitivity, cone sensitivity, and photoreceptor layer thickness in retinal degenerative diseases. Invest Ophthalmol Vis Sci. 2011;52(10):7141–7147. [PubMed: 21810977]
19. Crossland MD, Engel SA, Legge GE. The preferred retinal locus in macular disease: toward a consensus definition. Retina. 2011;31(10):2109–2114. [PubMed: 21555970]
20. Mukherjee D, Lad EM, Vann RR, et al. Correlation Between Macular Integrity Assessment and Optical Coherence Tomography Imaging of Ellipsoid Zone in Macular Telangiectasia Type 2. Invest Ophthalmol Vis Sci. 2017;58(6):Bio291–bio299.
21. Fuster-Garcia C, Garcia-Garcia G, Gonzalez-Romero E, et al. USH2A Gene Editing Using the CRISPR System. Mol Ther Nucleic Acids. 2017;8:529–541. [PubMed: 28918053]

22. Slijkerman RW, Vache C, Dona M, et al. Antisense Oligonucleotide-based Splice Correction for USH2A-associated Retinal Degeneration Caused by a Frequent Deep-intronic Mutation. Mol Ther Nucleic Acids. 2016;5(10):e381. [PubMed: 27802265]
23. Ferris FL 3rd, Kassoff A, Bresnick GH, Bailey I. New visual acuity charts for clinical research. Am J Ophthalmol. 1982;94(1):91–96. [PubMed: 7091289]
24. Williams TD, Wilkinson JM. Position of the fovea centralis with respect to the optic nerve head. Optom Vis Sci. 1992;69(5):369–377. [PubMed: 1594198]
25. Crossland MD, Dunbar HM, Rubin GS. Fixation stability measurement using the MP1 microperimeter. Retina. 2009;29(5):651–656. [PubMed: 19262440]
26. Chiu SJ, Izatt JA, O'Connell RV, Winter KP, Toth CA, Farsiu S. Validated Automatic Segmentation of AMD Pathology Including Drusen and Geographic Atrophy in SD-OCT Images. Invest Ophthalmol Vis Sci. 2012;53(1):53–61. [PubMed: 22039246]
27. Chiu SJ, Li XT, Nicholas P, Toth CA, Izatt JA, Farsiu S. Automatic segmentation of seven retinal layers in SDOCT images congruent with expert manual segmentation. Opt Express. 2010;18(18):19413–19428. [PubMed: 20940837]
28. Amidror I Scattered data interpolation methods for electronic imaging systems: a survey. J Electron Imaging. 2002;11(2):157–176.
29. Smith TB, Parker M, Steinkamp PN, et al. Structure-Function Modeling of Optical Coherence Tomography and Standard Automated Perimetry in the Retina of Patients with Autosomal Dominant Retinitis Pigmentosa. PLOS ONE. 2016;11(2):e0148022–e0148022.
30. Bland JM, Altman DG. Measuring agreement in method comparison studies. Stat Methods Med Res. 1999;8(2):135–160. [PubMed: 10501650]
31. Wu Z, Ayton LN, Guymer RH, Luu CD. Intrasession test-retest variability of microperimetry in age-related macular degeneration. Invest Ophthalmol Vis Sci. 2013;54(12):7378–7385. [PubMed: 24135753]
32. Charng J, Sanfilippo PG, Attia MS, et al. Interpreting MAIA Microperimetry Using Age- and Retinal Loci-Specific Reference Thresholds. Transl Vis Sci Technol. 2020;9(7):19.
33. Denniss J, Astle AT. Central perimetric sensitivity estimates are directly influenced by the fixation target. Ophthalmic Physiol Opt. 2016;36(4):453–458. [PubMed: 27146101]
34. Hufnagel RB, Liang W, Duncan JL, et al. Tissue-specific genotype-phenotype correlations among USH2A-related disorders in the RUSH2A study. Hum Mutat. 2022;43(5):613–624. [PubMed: 35266249]
35. Weingessel B, Sacu S, Vécsei-Marlovits PV, Weingessel A, Richter-Mueksch S, Schmidt-Erfurth U. Interexaminer and intraexaminer reliability of the microperimeter MP-1. Eye. 2009;23(5):1052–1058. [PubMed: 18670459]
36. Anastasakis A, McAnany JJ, Fishman GA, Seiple WH. Clinical value, normative retinal sensitivity values, and intrasession repeatability using a combined spectral domain optical coherence tomography/scanning laser ophthalmoscope microperimeter. Eye (Lond). 2011;25(2):245–251. [PubMed: 21178993]
37. Chen FK, Patel PJ, Xing W, et al. Test–Retest Variability of Microperimetry Using the Nidek MP1 in Patients with Macular Disease. Invest Ophthalmol Vis Sci. 2009;50(7):3464–3472. [PubMed: 19324853]
38. Wong EN, De Soyza JDA, Mackey DA, Constable IJ, Chen FK. Intersession Test-Retest Variability of Microperimetry in Type 2 Macular Telangiectasia. Transl Vis Sci Technol. 2017;6(6):7.
39. Chandramohan A, Stinnett SS, Petrowski JT, et al. Visual function measures in early and intermediate age-related macular degeneration. Retina. 2016;36(5):1021–1031. [PubMed: 26925551]
40. Johnson CA, Adams CW, Lewis RA. Fatigue effects in automated perimetry. Appl Opt. 1988;27(6):1030–1037. [PubMed: 20531515]
41. Cehajic-Kapetanovic J, Xue K, Martinez-Fernandez de la Camara C, et al. Initial results from a first-in-human gene therapy trial on X-linked retinitis pigmentosa caused by mutations in RPGR. Nat Med. 2020;26(3):354–359. [PubMed: 32094925]

42. MacLaren RE, Groppe M, Barnard AR, et al. Retinal gene therapy in patients with choroideremia: initial findings from a phase 1/2 clinical trial. Lancet. 2014;383(9923):1129–1137. [PubMed: 24439297]

43. Iftikhar M, Kherani S, Kaur R, et al. Progression of Retinitis Pigmentosa as Measured on Microperimetry: The PREP-1 Study. Ophthalmol Retina. 2018;2(5):502–507. [PubMed: 31047333]

44. Fleckenstein M, Charbel Issa P, Fuchs HA, et al. Discrete arcs of increased fundus autofluorescence in retinal dystrophies and functional correlate on microperimetry. Eye (Lond). 2009;23(3):567–575. [PubMed: 18344954]

45. Funatsu J, Murakami Y, Nakatake S, et al. Direct comparison of retinal structure and function in retinitis pigmentosa by co-registering microperimetry and optical coherence tomography. PLOS ONE. 2019;14(12):e0226097.

46. Charng J, Lamey TM, Thompson JA, et al. Edge of Scotoma Sensitivity as a Microperimetry Clinical Trial End Point in USH2A Retinopathy. Transl Vis Sci Technol. 2020;9(10):9–9.

47. Rangaswamy NV, Patel HM, Locke KG, Hood DC, Birch DG. A Comparison of Visual Field Sensitivity to Photoreceptor Thickness in Retinitis Pigmentosa. Invest Ophthalmol Vis Sci. 2010;51(8):4213–4219. [PubMed: 20220048]

48. Sallo FB, Peto T, Egan C, et al. The IS/OS Junction Layer in the Natural History of Type 2 Idiopathic Macular Telangiectasia. Invest Ophthalmol Vis Sci. 2012;53(12):7889–7895. [PubMed: 23092925]

49. Hartel BP, Lofgren M, Huygen PL, et al. A combination of two truncating mutations in USH2A causes more severe and progressive hearing impairment in Usher syndrome type IIa. Hear Res. 2016;339:60–68. [PubMed: 27318125]

50. Lenassi E, Vincent A, Li Z, et al. A detailed clinical and molecular survey of subjects with nonsyndromic USH2A retinopathy reveals an allelic hierarchy of disease-causing variants. Eur J Hum Genet. 2015;23(10):1318–1327. [PubMed: 25649381]

51. Folgar FA, Yuan EL, Farsiu S, Toth CA. Lateral and axial measurement differences between spectral-domain optical coherence tomography systems. J Biomed Opt. 2014;19(1):16014.

Health Research Alliance Author Manuscript

Health Research Alliance Author Manuscript

Highlights

- Baseline microperimetry and spectral domain OCT were analyzed in the RUSH2A study.
- Better BCVA and larger CST were associated with larger EZ area.
- Longer disease duration correlated with more severe structure-function abnormalities.
- Monitoring these changes will provide important insights into disease mechanisms.

Health Research Alliance Author Manuscript

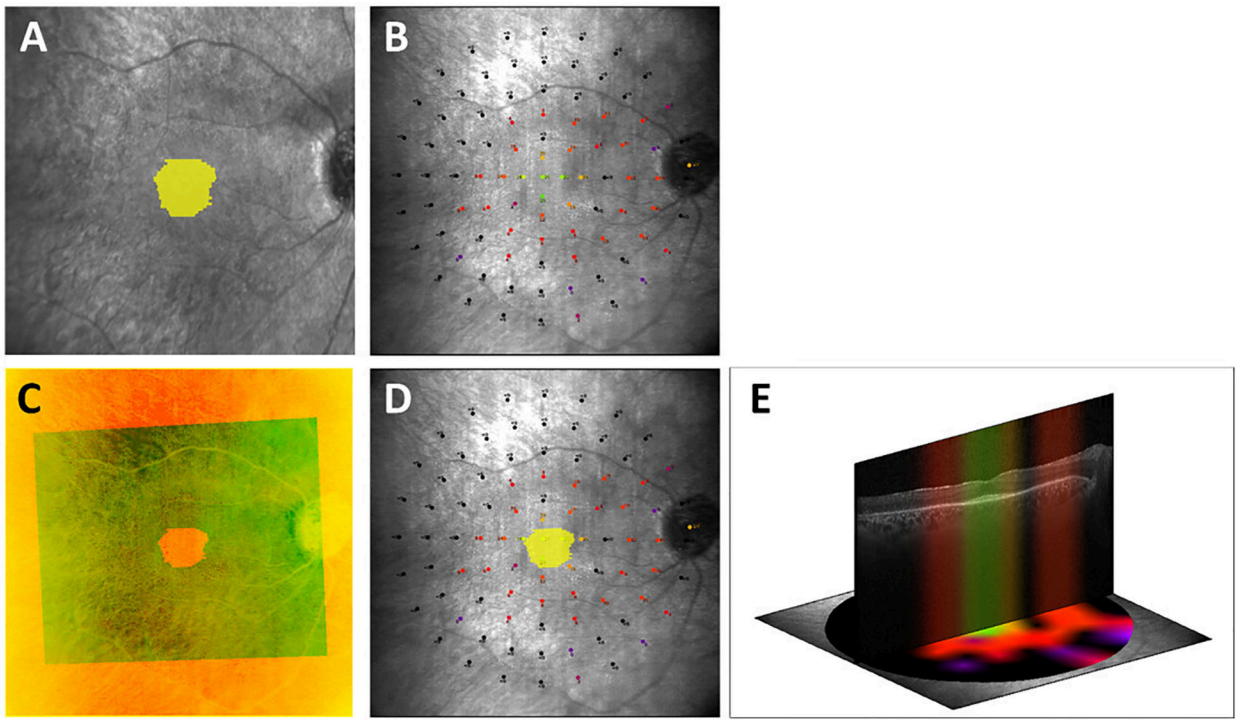

Figure 1. Example of microperimetry-OCT overlay.

Figure 1: A. Intact ellipsoid zone (EZ) area segmented on SD-OCT images (yellow) mapped onto the infrared reflectance (IR) image simultaneously acquired during OCT imaging. **B.** Microperimetry image. **C.** IR image acquired simultaneously with SD-OCT image (smaller field of view) registered to the microperimetry fundus image (larger field of view). The near-perfect vessel overlap between the images qualitatively demonstrates the accuracy of the registration. **D.** Intact EZ area (yellow) mapped onto the microperimetry image. **E.** Central OCT B-scan with the corresponding sensitivity profile as obtained from the interpolated microperimetry map demonstrates structure-function correlation.

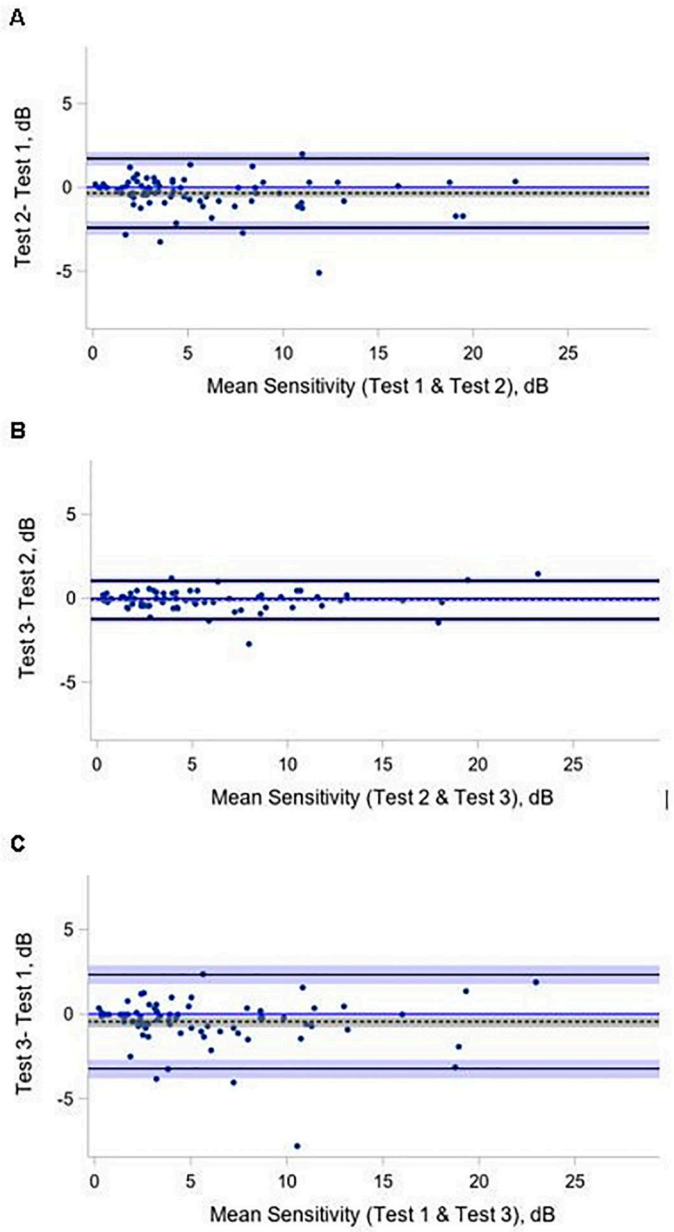

Figure 2 (A-C). Bland-Altman plots of mean retinal sensitivity on microperimetry.

Bland-Altman plot of tests 1, 2, and 3 pairwise comparisons. The analysis included participants with 3 gradable fields (N=78). The differences between test 1 and 2, test 2 and 3, test 1 and 3 for mean retinal sensitivity (dB) are plotted on the y-axis against their averages on the x-axis. Limits of Agreement are shown as solid, black lines with 95% confidence intervals (light blue areas), bias (as dotted black line) with 95% confidence interval (gray area).

Health Research Alliance Author Manuscript

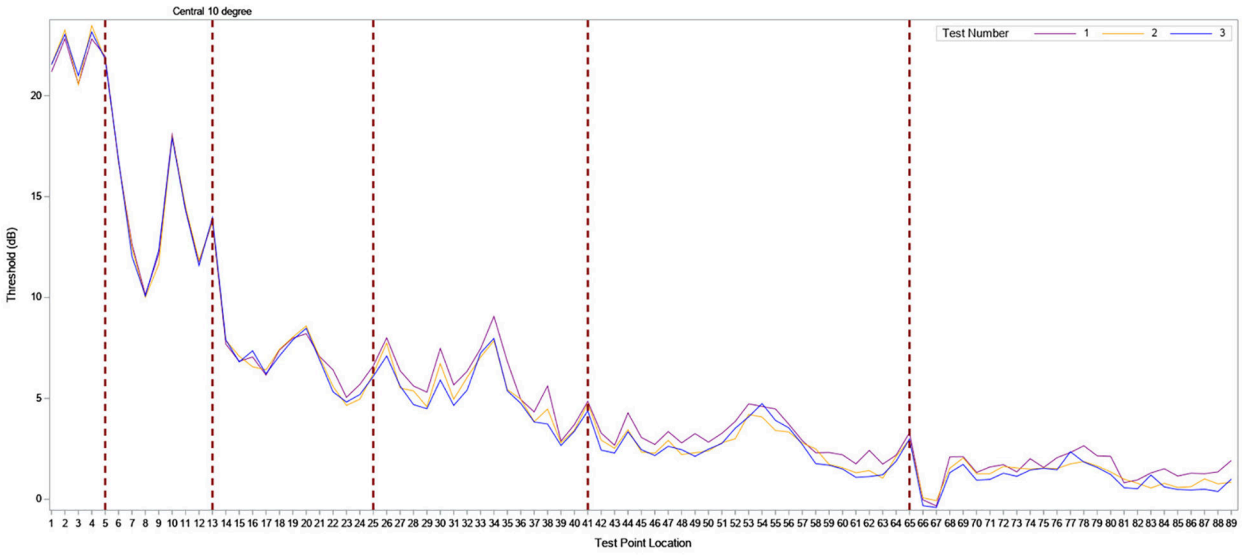

Figure 3. Point-wise sensitivity analysis.

The ID numbers corresponding to MP grid loci are listed along the X axis, and retinal sensitivity for each locus ID (dB) on the y axis. Foveal center= ID number 1; central 10 degree = ID numbers 1–13 (demarcated by the dotted red line).

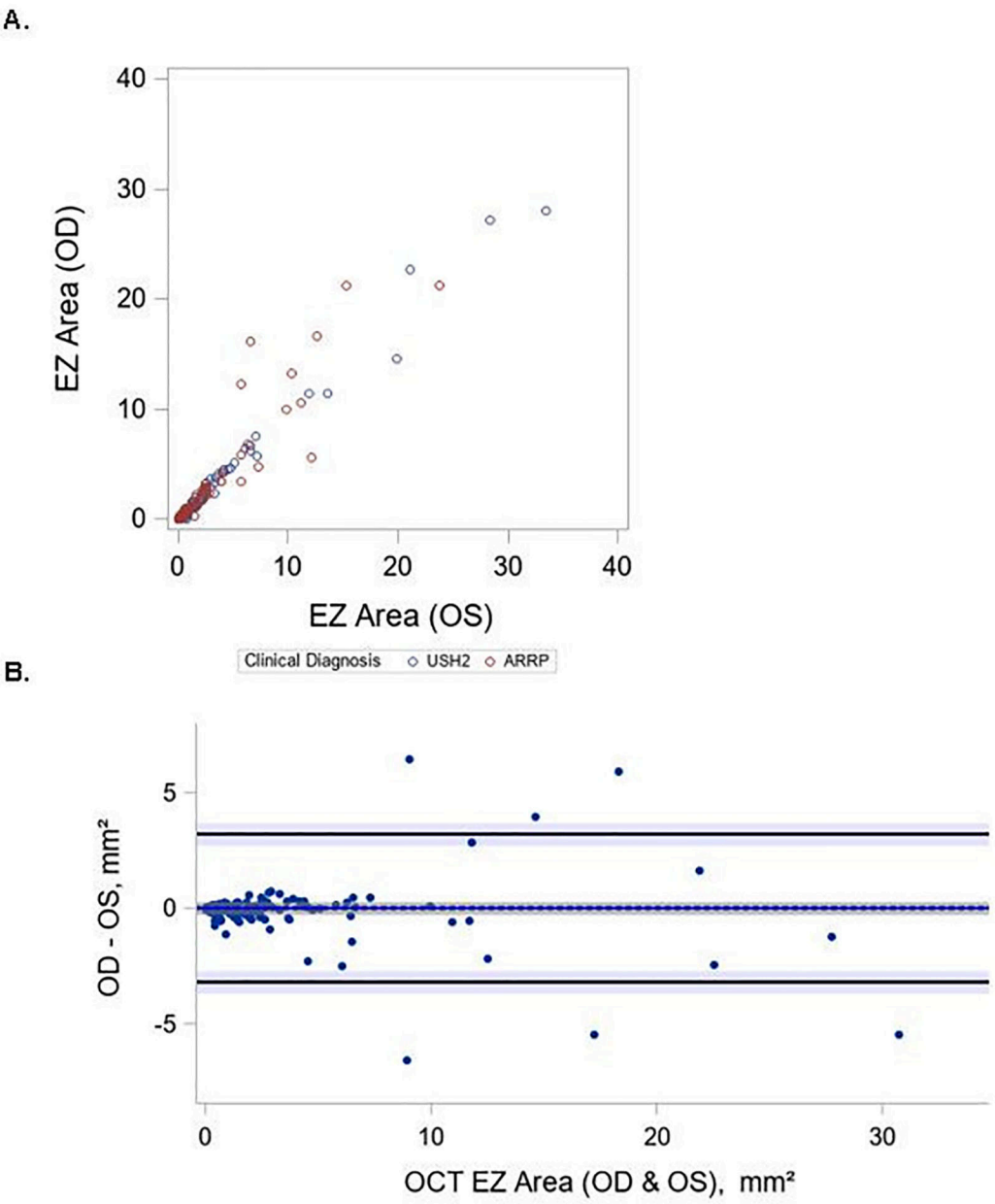

Figure 4 (A-B). Interocular variability and symmetry of OCT EZ area.

Bland-Altman plot of OCT EZ area measurements from the left and right eye of each participant. The difference in OCT EZ between left and right eyes for OCT EZ is plotted on the y-axis against their averages on the x-axis. ICC=0.96 with 95%CI (0.94, 0.97) A. Scatter plot of OCT EZ area measurements from left and right eye of each participant B. Bland-Altman plot of OCT EZ area measurements from left and right eye of each participant

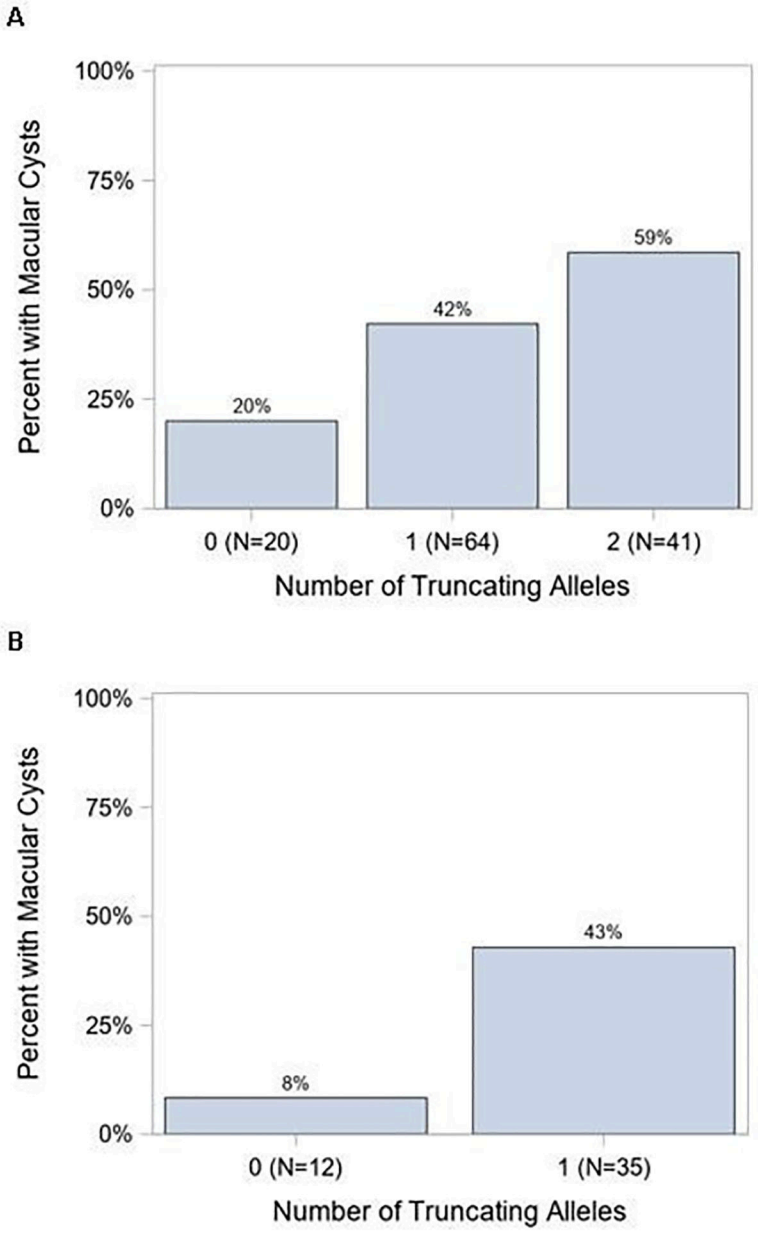

Figure 5 (A-B). Macular cyst correlation with truncating USH2A alleles.

(A) Proportion of patients with macular cysts in the RUSH2A cohort who have 0, 1, or 2 truncating alleles (p = 0.03). (B) Similar analysis for the ARRP subgroup (p-value = 0.05).

Health Research Alliance Author Manuscript

Figure 6. Retinal sensitivities outside the intact EZ are higher with nonsyndromic-associated missense alleles.

Subgroup analysis of patients with 1 truncating allele and 1 missense allele in the nonsyndromic-associated (RP-enriched) group or other. RP-enriched missense alleles include p.Cys759Phe, p.Cys3294Trp, and p.Cys3358Tyr[34].

Table 1.

Baseline participant characteristics for microperimetry analysis cohort, overall and by clinical diagnosis.

Characteristic	Overall	Clinical Diagnosis	
	N=87	USH2 N= 52	ARRP N= 35
Gender			
Female	48 (55%)	29 (56%)	19 (54%)
Male	39 (45%)	23 (44%)	16 (46%)
Race/Ethnicity			
White	79 (91%)	48 (92%)	31 (88%)
Hispanic	5 (6%)	3 (6%)	2 (6%)
Asian	3 (3%)	1 (2%)	2 (6%)
Enrollment area			
United States/Canada	49 (56%)	28 (54%)	21 (60%)
Europe/UK	38 (44%)	24 (46%)	14 (40%)
Age at enrollment, yrs [a]			
Median (IQR)	37 (28, 45)	34 (26, 42)	38 (35, 48)
[Min, Max]	[15, 80]	[15, 80]	[24, 75]
<35	35 (40%)	27 (52%)	8 (23%)
35–45	31 (36%)	16 (31%)	15 (43%)
>=45	21 (24%)	9 (17%)	12 (34%)
Age of onset, yrs [b]			
Median (IQR)	20 (14, 29)	16 (13, 22)	29 (19, 41)
[Min, Max]	[5, 65]	[5, 46]	[7, 65]
<16	29 (34%)	24 (46%)	5 (15%)
[16, 25)	28 (33%)	20 (38%)	8 (24%)
>=25	29 (34%)	8 (15%)	21 (62%)
Duration of Disease, yrs [b]			
Median (IQR)	12 (6, 20)	15 (8, 23)	10 (6, 17)
[Min, Max]	[1, 60]	[1, 60]	[1, 36]
<10	31 (36%)	15 (29%)	16 (47%)
[10, 19)	34 (40%)	19 (37%)	15 (44%)
>=20	21 (24%)	18 (35%)	3 (9%)
Severity of hearing loss [c]			
Normal	29 (35%)	0	29 (83%)
Mild	7 (8%)	2 (4%)	5 (14%)
Moderate	37 (45%)	36 (75%)	1 (3%)
Severe/Profound	10 (12%)	10 (21%)	0
Smoking status			

Characteristic	Overall	Clinical Diagnosis	
	N=87	USH2 N= 52	ARRP N= 35
Yes	25 (29%)	15 (29%)	10 (29%)
No	62 (71%)	37 (71%)	25 (71%)
Current use of dietary supplements			
None	42 (48%)	31 (60%)	11 (31%)
Vitamin A only	6 (7%)	3 (6%)	3 (9%)
DHA only	4 (5%)	3 (6%)	1 (3%)
Lutein only	5 (6%)	2 (4%)	3 (9%)
Combination of 3	30 (34%)	13 (25%)	17 (49%)

[a] 28 participants were not permitted to report date of birth due to regulatory restrictions. Therefore, only year of birth and categorical age was reported. For those participants, July 1st with the reported birth year was imputed as birth date to calculate continuous age

[b] 1 participant in the ARRP group was missing age of onset (a participant-reported field based on their awareness of visual symptoms) and duration of disease (computed based on age of onset and date of enrollment)

[c] Composite score based on 4F-PTA (four frequency air conduction threshold pure-tone average based on 0.5, 1, 2, and 4 kHz). 5 participants in the USH2 group were missing baseline 4F-PTA (3 had cochlear implants in both ears, 2 missed their audiology exam for other reasons)

Table 2.

Baseline microperimetry metrics, overall and by clinical diagnosis

	Overall N = 87	Clinical Diagnosis	
		USH2 N= 52	ARRP N= 35
Mean retinal sensitivity[a,b]			
Mean (SD)	5.9 (5.0)	5.4 (5.0)	6.7 (5.1)
Median (IQR)	4.2 (2.3, 8.5)	3.5 (2.1, 8.4)	5.1 (2.9, 9.0)
[Min, Max]	[0.0, 22.2]	[0.0, 22.2]	[0.6, 19.5]
95% BCEA area [a]			
Mean (SD)	3.8 (8.7)	4.8 (10.9)	2.4 (2.9)
Median (IQR)	1.5 (0.8, 2.8)	1.3 (0.8, 2.8)	1.7 (0.8, 2.8)
[Min, Max]	[0.2, 57.2]	[0.2, 57.2]	[0.2, 15.5]
Number of loci >25 dB [c]			
Median (IQR)	2 (0, 4)	1 (0,3)	2 (0, 5)
[Min, Max]	[0, 31]	[0, 31]	[0, 21]
Number of loci 15–25 dB [c]			
Median (IQR)	8 (6, 21)	7 (5, 21)	10 (7, 21)
[Min, Max]	[1, 81]	[1, 54]	[4, 81]
Number of loci 0–14 dB [c]			
Median (IQR)	30 (18, 42)	32 (17, 42)	27 (19, 41)
[Min, Max]	[1, 63]	[1,58]	[4, 63]
Number of loci with absolute scotoma (<0 dB) [c]			
Median (IQR)	44 (22, 59)	46 (23, 63)	43 (22, 56)
[Min, Max]	[1, 83]	[1, 83]	[1, 80]
Fixation stability			
Stable on any tests	86 (99%)	51 (98%)	35 (100%)
Unstable on all tests	1 (1%)	1 (2%)	0
Foveal involvement			
Yes on any tests	73 (84%)	48 (92%)	25 (71%)
No on all tests	14 (16%)	4 (8%)	10 (29%)

[a]Using the average of first and/or second tests

[b]One participant has ungradable mean retinal sensitivity

[c]Using the average of test 1 and test 2 (based on raw data)

Table 3.

Mean sensitivity stratified by baseline participant characteristics, overall and by clinical diagnosis

	All		USH2		ARRP		Univariable	Multivariable
Characteristic	**N=87**[a]	**MS Median (IQR), dB**	**N=52**	**MS Median (IQR), dB**	**N=35**	**MS Median (IQR), dB**	**P value**	**P value**[b]
Gender							0.35	NA
Female	48	4.8 (2.8, 9.4)	29	4.2 (2.6, 10.4)	19	5.6 (3.0, 9.8)		
Male	39	3.4 (2.1, 7.9)	23	3.3 (1.7, 7.6)	16	4.4 (2.7, 8.6)		
Race/Ethnicity							0.62	NA
White	79	4.1 (2.3, 8.6)	48	3.3 (2.0, 8.2)	31	5.6 (2.9, 9.8)		
Hispanic	5	5.1 (2.1, 6.0)	3	5.1 (2.1, 8.3)	2	4.0 (2.1, 6.0)		
Asian	3	4.4 (3.5, 19.1)	1	19.1	2	3.9 (3.5, 4.4)		
Age at enrollment, yrs							0.13	NA
<35	35	3.5 (2.5, 8.5)	27	3.4 (2.3, 8.6)	8	4.6 (2.9, 7.1)		
35–45	31	4.2 (2.1, 8.2)	16	4.1 (2.1, 9.0)	15	4.4 (2.1, 8.2)		
≥45	21	4.2 (2.7, 9.0)	9	3.3 (0.4, 4.2)	12	7.9 (3.3, 10.5)		
Duration of Disease, yrs							**0.004**	**0.01**
<10	31	7.0 (3.4, 10.8)	15	8.3 (3.2, 10.8)	16	5.4 (3.6, 10.4)		
[10,20)	34	2.8 (1.9, 6.0)	19	2.3 (1.5, 4.8)	15	2.9 (1.9, 6.6)		
>=20	21	4.1 (2.1, 7.6)	18	3.8 (1.7, 4.8)	3	11.3 (4.4, 11.4)		
Smoking status							0.73	NA
Yes	25	3.8 (2.1, 7.6)	15	3.4 (1.5, 7.6)	10	4.0 (2.8, 11.0)		
No	62	4.2 (2.5, 8.5)	37	3.5 (2.1, 8.5)	25	5.6 (3.0, 8.4)		
Current use of dietary supplements						0.61	NA	
None	42	4.2 (2.6, 8.6)	31	4.2 (2.6, 8.3)	11	5.8 (3.3, 11.3)		
Vitamin A only	6	2.2 (1.9, 6.6)	3	1.9 (1.7, 2.3)	3	6.6 (2.1, 9.8)		
DHA only	4	2.4 (1.2, 4.6)	3	2.9 (0.5, 6.2)	1	1.9		
Lutein only	5	7.6 (1.3, 8.2)	2	5.9 (1.3, 10.5)	3	7.6 (0.6, 8.2)		
Combination	30	4.2 (2.7, 9.1)	13	3.5 (2.1, 11.0)	17	4.6 (3.0, 7.5)		

[a] One participant has ungradable mean retinal sensitivity.

[b] Multivariable model adjusted for clinical diagnosis ($P = 0.55$) and other factors included in final model as noted.

Table 4.

Correlation of baseline mean sensitivity with other functional and structural measures

Function al or Structural Measure	Overall		Clinical Diagnosis	Clinical Diagnosis	Clinical Diagnosis	Clinical Diagnosis	Spearman Correlation Coefficient (95% Cl)	P-Value
			USH2		ARRP			
	N=87[a]	Median (IQR)	N=52	Median (IQR)	N=35	Median (IQR)		
VAETDRS letter score (approx. Snellen equivalent)							0.34 (0.13, 0.51)	0.001
<68 (<20/40)	6	4.0 (3.0, 9.1)	5	3.3 (3.0, 4.8)	1	11.3		
69–73 (20/40)	5	2.1 (1.7, 5.1)	3	1.7 (0.0, 2.1)	2	6.7 (5.1, 8.2)		
74–78 (20/32)	17	2.8 (2.1, 4.2)	13	2.8 (2.3, 4.2)	4	2.5 (1.9, 3.7)		
79–83 (20/25)	25	4.1 (2.6, 7.0)	11	3.5 (0.07, 5.1)	14	5.2 (3.3, 7.6)		
>=84 (>=20/20)	34	8.1 (2.7, 11.4)	20	8.4 (3.0, 11.9)	14	5.8 (2.7, 11.4)		
OCT EZ area (mm^2)[b]							0.68 (0.55, 0.78)	<0.001
[0,1)	22	2.1 (0.7, 4.2)	16	1.9 (0.5, 3.4)	6	3.6 (1.9, 8.2)		
[1,4)	38	3.2 (2.5, 5.1)	23	3.2 (2.3, 5.1)	15	3.3 (2.5, 5.6)		
>=4	26	9.2 (6.6, 12.9)	13	10.8 (8.3, 12.9)	13	7.6 (6.0, 11.4)		
Central subfield thickness[c] (um)							0.37 (0.17, 0.54)	<0.001
<230	19	2.3 (0.7, 4.2)	15	1.7 (0.5, 3.5)	4	6.3 (3.6, 9.8)		
[230, 250)	14	3.8 (1.9, 7.0)	9	4.8 (2.1, 7.0)	5	3.5 (1.8, 4.2)		
[250, 280)	23	3.8 (2.8, 7.9)	11	6.2 (2.8, 10.5)	12	3.6 (2.7, 7.0)		
>=280	30	6.8 (2.9, 11.0)	16	6.5 (2.8, 10.9)	14	6.8 (4.6, 16.1)		

[a] One participant has ungradable mean retinal sensitivity.

[b] 1 participant has EZ beyond scan area and therefore ungradable.

[c] CST was missing for 1 participant.

Table 5.

Baseline OCT features, overall and by clinical diagnosis.

	Overall	**Clinical Diagnosis**	
	N = 127	**USH2 N= 80**	**ARRP N= 47**
Cyst			
None	70 (55%)	39 (49%)	31 (66%)
Outside the central 1 mm only	18 (14%)	13 (16%)	5 (11%)
Inside the central 1 mm only	6 (5%)	4 (5%)	2 (4%)
Both inside and outside the central 1 mm	31 (24%)	22 (28%)	9 (19%)
Ungradable	2 (2%)	2 (3%)	0
Definite vitreomacular traction with deformation within central 1mm			
Yes	1 (1%)	1 (1%)	0
No	123 (97%)	76 (95%)	47 (100%)
Ungradable	3 (2%)	3 (4%)	0
Definite epiretinal membrane with deformation within central 1mm			
Yes	25 (20%)	13 (16%)	12 (26%)
No	100 (79%)	65 (81%)	35 (74%)
Ungradable	2 (2%)	2 (3%)	0
OCT EZ area[a] (mm^2)			
Median (IQR)	1.5 (0.5, 3.5)	1.4 (0.4, 3.1)	2.3 (0.7, 5.7)
[Min, Max]	[0.0, 33.4]	[0.0, 33.4]	[0.0, 21.3]
Mean (SD)	3.6 (5.6)	3.1 (5.7)	4.3 (5.6)
Central subfield thickness(um)			
Median (IQR)	253 (228, 285)	247 (223, 280)	261 (246, 288)
[Min, Max]	[137, 519]	[137, 519]	[175, 323]
Mean (SD)	257 (50)	253 (57)	264 (33)

[a] 1 participant has EZ beyond scan area and therefore ungradable.

Table 6.

Baseline participant characteristics by presence of cysts on OCT.

		Presence of cysts[a]			
Characteristic					
N=70	**N=125**	**None**	**Outside central 1mm only N=18**	**Inside central 1mm N=37**	**P-value**
Clinical diagnosis					0.22
USH2	78	39 (50%)	13 (17%)	26 (33%)	
ARRP	47	31 (66%)	5 (11%)	11 (23%)	
Foveal involvement [b]					0.60
Yes	56	32 (56%)	6 (11%)	19 (33%)	
No	14	8 (57%)	2 (14%)	4 (29%)	
Possible	18	13 (72%)	0	5 (28%)	
EZ area (mm^2)	124				0.29
Median (IQR)		1.4 (0.6, 4.3)	1.0 (0.2, 2.6)	1.9 (0.7, 3.2)	
[Min, Max]		[0.0, 33.4]	[0.0, 11.2]	[0.0, 14.5]	
Central subfield thickness [c]	124				**<0.001**
Median (IQR)		252 (226, 279)	238 (225, 280)	271 (247, 300)	
[Min, Max]		[148, 323]	[137, 323]	[212, 519]	
95% BCEA area	88				0.61
Median (IQR)		1.5 (0.8, 2.8)	1.2 (0.7, 2.3)	1.5 (0.8, 2.9)	
[Min, Max]		[0.2, 57.2]	0.5, 2.8]	[0.5, 16.8]	
VA	125				**0.01**
Median					
(IQR)		83 (75, 87)	75 (69, 82)	79 (75, 83)	
[Min, Max]		[43.0, 94.0]	[18.0, 88.0]	[41, 92]	
Definite VMT with deformation within center 1mm					0.35
Yes	1	0	0	1 (100%)	
No	123	70 (57%)	18 (15%)	35 (28%)	
Ungradable	1	0	0	1 (100%)	
Definite ERM with deformation within center 1mm					0.19
Yes	25	12 (48%)	2 (8%)	11 (44%)	
No	100	58 (58%)	16 (16%)	26 (26%)	

[a] 2 participants with ungradable cysts were excluded from this analysis

[b] Foveal involvement was not available for 37 participants

[c] CST was missing for 1 participant

Table 7.

OCT EZ area stratified by baseline participant characteristics, overall and by clinical diagnosis

Characteristic	All		Clinical Diagnosis				*Univariable a*	*Multivariable b*
			USH2		ARRP			
	N=126	EZ Area Median (IQR), mm^2	N=80	EZ Area Median (IQR), mm^2	N=46	EZ Area Median (IQR), mm^2	*P-value*	*P-value*
Gender							0.63	
Female	68	1.8 (0.4, 4.4)	44	1.8 (0.3, 3.8)	24	2.0 (0.6, 5.2)		
Male	58	1.4 (0.6, 3.4)	36	1.2 (0.4, 2.2)	22	2.3 (1.0, 5.7)		
Race/Ethnicity							0.93	
White	112	1.5 (0.5, 3.4)	70	1.4 (0.4, 3.0)	42	2.3 (0.7, 5.7)		
Hispanic	9	1.6 (1.0, 5.1)	7	1.4 (0.4, 5.1)	2	3.6 (1.6, 5.7)		
Asian	5	1.1 (0.3, 2.8)	3	1.1 (0.0, 11.4)	2	1.6 (0.3, 2.8)		
Age at enrollment, yrs							<0.001	
<35	44	2.6 (1.4, 5.9)	36	2.6 (1.4, 5.6)	8	2.6 (2.0, 6.2)		
35–45	44	1.4 (0.6, 2.6)	25	1.2 (0.4, 2.1)	19	1.6 (0.7, 3.5)		
45 years or older	38	0.6 (0.1, 2.8)	19	0.2 (0.0, 0.7)	19	1.8 (0.5, 9.9)		
Duration of Disease, yrs [c]							**<0.001**	**<0.001**
<10	36	4.5 (2.5, 8.5)	20	4.6 (2.6, 6.8)	16	3.9 (2.0, 14.7)		
[10,20)	46	1.6 (0.7, 2.8)	25	1.6 (0.7, 2.5)	21	1.6 (0.7, 2.8)		
>=20	43	0.6 (0.1, 1.3)	35	0.6 (0.1, 1.3)	8	0.5 (0.0, 1.5)		
Smoking status							0.79	
Yes	32	1.7 (0.5, 2.6)	20	1.8 (0.5, 2.5)	12	1.7 (0.6, 3.2)		
No	94	1.4 (0.5, 4.3)	60	1.3 (0.4, 3.4)	34	2.5 (0.9, 5.7)		
Current use of dietary supplements							0.87	
None	52	2.0 (0.7, 3.4)	41	1.9 (0.4, 3.3)	11	2.5 (1.0, 3.4)		
Vitamin A only	11	1.3 (0.5, 1.8)	5	0.8 (0.8, 1.3)	6	1.7 (0.5, 11.2)		
DHA only	5	0.7 (0.7, 1.5)	3	1.5 (0.7, 2.5)	2	0.6 (0.5, 0.7)		
Lutein only	9	1.4 (0.7, 4.7)	5	1.6 (1.4, 4.7)	4	1.0 (0.4, 3.5)		
Combination	49	1.3 (0.4, 4.8)	26	0.7 (0.2, 3.0)	23	2.6 (0.9, 9.9)		

[a] Numeric factors were analyzed using continues version.

[b] Multivariable model adjusted for clinical diagnosis ($P = 0.75$) and other factors included in final model as noted

[c] 1 participant in the ARRP group was missing age of onset (a participant-reported field based on their awareness of visual symptoms) and duration of disease (computed based on age of onset and date of enrollment)

Table 8.

Correlation of baseline OCT EZ area with other functional and structural measurements

Factors to Evaluate	**a) All**	**Clinical Diagnosis**	**Spearman Correlation Coefficient (95% CI)**					**P-value**[a]
	N=126	**OCT EZ Area – Median (IQR)**	**N=80**	**USH2**	**N=46**	**ARRP**		
VA ETDRS letter score (approx. Snellen equivalent)							0.61 (0.48, 0.71)	<0.001
<68 (<20/40)	14	0.0 (0.0, 0.2)	11	0.0 (0.0, 0.6)	3	0.0 (0.0, 0.0)		
69–73 (20/40)	14	0.3 (0.2, 0.7)	9	0.2 (0.2, 0.4)	5	0.7 (0.3, 0.7)		
74–78 (20/32)	24	1.4 (0.8, 2.0)	17	1.4 (0.8, 2.1)	7	1.0 (0.5, 1.6)		
79–83 (20/25)	33	2.1 (0.8, 3.5)	18	1.3 (0.4, 2.6)	15	2.8 (2.1, 5.7)		
>=84 (>=20/20)	41	3.4 (1.4, 7.2)	25	3.7 (1.4, 7.2)	16	3.0 (1.3, 9.5)		
Central subfield thickness[b] (μm)							0.67 (0.57, 0.76)	<0.001
<230	33	0.3 (0.1, 0.7)	28	0.4 (0.2, 0.8)	5	0.1 (0.0, 0.2)		
[230, 250)	22	1.4 (0.7, 2.6)	13	1.9 (0.8, 2.6)	9	1.0 (0.7, 1.6)		
[250, 280)	33	2.1 (0.9, 4.7)	18	1.8 (0.9, 3.7)	15	2.5 (0.9, 5.7)		
>=280	37	3.4 (1.8, 7.2)	20	3.4 (1.7, 6.9)	17	4.3 (2.1, 9.9)		
Spherical equivalent[c]							−0.13 (−0.31, 0.05)	0.16
< −3.25	27	1.3 (0.4, 2.8)	19	1.4 (0.4, 3.0)	8	1.2 (0.5, 2.4)		
[−3.25, −1.125)	26	2.6 (1.2, 5.1)	19	2.5 (1.2, 4.5)	7	3.5 (0.7, 9.9)		
[−1.125, −0.125)	28	1.5 (0.8, 5.5)	15	1.1 (0.3, 3.7)	13	2.6 (1.4, 6.8)		
>= −0.125	30	1.0 (0.2, 2.6)	19	0.7 (0.1, 2.5)	11	1.6 (0.5, 2.7)		

[a]Numeric factors were analyzed using continues version

[b]CST was missing for 1 participant

[c]Spherical equivalent was missing for 15 participants

Table 9.

Baseline MP-OCT overlay metrics, overall and by clinical diagnosis and disease duration.

	All	Clinical Diagnosis		P-value	Disease duration[b]			P-value
	N	USH2	ARRP		<10	10–20	≥20	
	N= 83	N=51	N=32		N= 29	N=34	N=19	
Average sensitivity within Intact EZ Area				0.17				0.08
Median (Q1, Q3)	23 (21, 25)	22 (21, 25)	24 (22, 25)		22 (21, 25)	24 (22, 25)	20 (18, 24)	
Average sensitivity (interpolated) within intact EZ area				0.13				0.02
Median (Q1, Q3)	21 (19, 24)	21 (18, 23)	22 (20, 24)		21 (19, 24)	21 (20, 23)	18 (15, 23)	
Average sensitivity outside intact EZ area				0.80				0.02
Median (Q1, Q3)	2 (1, 6)	2 (1, 7)	2 (2, 5)		4 (2, 8)	2 (1, 4)	3 (1, 5)	
Average sensitivity (interpolated) outside intact EZ Area				0.64				0.01
Median (Q1, Q3)	2 (1, 5)	2 (1, 5)	2 (1, 4)		3 (2, 6)	1 (1, 3)	2 (0, 4)	
Number of pixels within intact EZ area within the interpolated microperimetry map [a]				0.03				<0.001
Median (Q1, Q3)	21 (10, 43)	16 (6, 36)	24 (14, 60)		37 (23, 62)	16 (10, 34)	7 (3, 16)	
Number of pixels outside intact EZ area within the interpolated microperimetry map [a]				0.04				<0.001
Median (Q1, Q3)	713 (691, 724)	718 (699, 728)	710 (675, 720)		696 (673, 711)	718 (701, 725)	728 (715, 731)	
Number of sensitivity points within intact EZ area				0.03				<0.001
Median (Q1, Q3)	5 (3, 9)	4 (2, 8)	6 (4, 12)		9 (5, 12)	4 (2, 7)	2 (1, 4)	
Ratio of average sensitivity (interpolated) inside vs outside intact EZ				0.11				0.95
Median (Q1, Q3)	8 (3, 16)	6 (2, 15)	11 (5, 17)		6 (3, 13)	16 (4, 18)	6 (3, 13)	

[a] Different scale (all values reported have been divided by 1000)

[b] 1 participant in the ARRP group was missing age of onset (a participant-reported field based on their awareness of visual symptoms) and duration of disease (computed based on age of onset and date of enrollment